

# A Disc-Corona Model for a Rotating Black Hole

Xiao-Long Gong<sup>1\*</sup>, Li-Xin Li<sup>2</sup> and Ren-Yi Ma<sup>3</sup>

<sup>1</sup> Department of astronomy, Beijing Normal University, Beijing, 100875, P. R. China

<sup>2</sup> Kavli Institute for Astronomy and Astrophysics, Peking University, Beijing, 100875, P. R. China

<sup>3</sup> School of Physic and Mechanical & Electrical Engineering, Xiamen University, Xiamen, 361005, P. R. China

## ABSTRACT

We propose a disc-corona model in which a geometrically thin, optically thick disc surrounds a Kerr black hole, and magnetic fields exert a time-steady torque on the inner edge of the accretion disc. The analytical expression of the total gravitational power is derived from the thin-disc dynamics equations by using this new boundary condition. It is shown that the magnetic torque can considerably enhance the amount of energy released in the disc-corona system. Furthermore, the global solutions of this disc-corona system are obtained numerically. We find that the fraction of the power dissipated into the corona in the total for such disc-corona system increases with the increasing dimensionless black hole spin parameter  $a_*$ , but is insensitive on the  $\Delta\epsilon$  which is the additional radiative efficiency parameter relevant to magnetic torque, for  $\Delta\epsilon > 1$ . In addition, the emerged spectra from this disc-corona system are simulated by using Monte-Carlo method, and the effect of the different parameters on the output spectra is discussed.

**Key words:** accretion, accretion discs - black hole physics - magnetic fields

## 1 INTRODUCTION

It is believed that the black hole (BH) accretion disc is an effective model for explaining the high energy radiation in astrophysics. The standard accretion disc (SSD) model was proposed by Shakura & Sunyaev (1973), in which the disc is geometrically thin and optically thick. The SSD is widely used in modeling the spectral energy distribution (SED) of AGN. The general relativistic SSD model has been investigated in detail by Novikov & Thorne (1973, hereafter NT73), and Page & Thorne (1974, hereafter PT74). In this SSD model, it has been assumed that there is no stress at disc's inner edge, i.e. the so-called “no-torque inner boundary condition”.

However, the “no-torque inner boundary condition” was questioned by Krolik (1999) on the basis that magnetic fields are the likely agent of the torque in the discs (Balbus & Hawley 1998). Agol & Krolik (2000) proposed that magnetic fields connecting the disc to the plunging region can exert stresses on the inner edge of an accretion disc around a black hole, and they recomputed the relativistic corrections to the thin-disc dynamics equations when these stresses take the form of a time-steady torque on the inner edge of the disc. Gammie & Charles (1999) also noted that, within the confines of a highly-idealized model of inflow dynamics, this torque can considerably enhance the amount of energy released in the disc.

Apart from SSD, advection dominated accretion flow (ADAF) is another important model of the accretion flow (Narayan & Yi

1994, 1995). It is believed that black hole X-ray binaries present various spectral states, most notably the low/hard state, high/soft state and intermediate state. The SSD has been very successful in describing the high /soft states of Galactic black hole candidates (GBHCs), but their low/hard state characterized by power-law-type spectra was problematic to the SSD. The ADAF model is quite successful in reproducing the hard spectra of GBHCs, as well as those of low-luminosity AGNs (LLAGNs), however it also has a several problems. Thus we cannot expect to interpret the various components of spectra based on one accretion mode.

The power-law spectra of GBHCs is generally explained by Comptonization of softer photons by hot electrons from a magnetic corona on an accretion disc. Liang & Price (1977) proposed a high-temperature corona model analogous to solar corona, and the effects on the disc when part of the dissipation occurs in the corona were first discussed by Ionson & Kuperus (1984). In the accretion disc-corona scenario, an optically thin hot thermal corona is located above the surface of disc. A fraction of soft photons, which are from the cold disc, are Compton up-scattered to X-ray photon by hot electrons. In this model the corona can explain the power-law X-ray spectra very well, and reprocessing of the coronal X-rays by the cold disc gives rise to the observed emission lines naturally. The iron  $K_\alpha$  fluorescence line provides us a diagnostic of the geometry of the accretion flow and the property of the space-time around the BH. Recent work on the disc-corona model can be found in, e.g. Merloni & Fabian (2002); Liu et al. (2002); Cao (2008).

Shakura & Sunyaev (1973) used the famous “ $\alpha$ -prescription” to deal with viscosity, but the physical process leading to viscosity and turbulence in the disc remain unclear. The magnetic rota-

\* E-mail: gongxiaolong@mail.bnu.edu.cn

tion instability (MRI) of weak magnetic fields in accretion discs is thought to play an important role in the evolution and dynamics of astrophysical accretion discs. Balbus & Hawley (1998) argued that this instability should have a rapid growth rate of the order of the orbital frequency  $\Omega$ , resulting in a greatly-enhanced effective viscosity that is able to transport angular momentum outward. On the other hand, the magnetic fields generated in the SSD are strongly buoyant, and a fraction of the magnetic energy is transported vertically to heat the corona above the disc.

The multi-wavelength observations of nearby LLAGNs have revealed that the SEDs of LLAGNs and of GBHCs in the low/hard state possess many similarities, e.g. flat, compact radio cores with high brightness temperatures, and a hard X-ray power-law with high a energy cut-off. Merloni & Fabian (2002) pointed out that there should be a common accretion mode for these low luminosity black holes, and proposed a new model for low-luminosity black holes, in which a SSD at low accretion rates dissipates a large fraction of its gravitational energy in a magnetic corona.

Motivated by the these results, in this paper we shall investigate a disc-corona model, in which a geometrically thin, optically thick disc surrounds a rotating Kerr BH, a magnetic field connecting the plunging region and the disc exerts a non-zero torque at the inner boundary of the disc, and the corona is assumed to be heated by the reconnection of the magnetic fields generated by buoyancy instability in the disc. This paper is organized as follows. We describe the model in section 2, where in a magnetic torque is exerted on the inner edge of the accretion disc. In section 3 the global solutions of this disc-corona system are obtained, and the effects of different parameters on the fraction of accretion power dissipated into the corona are discussed. In section 4 we simulate the emerged spectra by using a Monte Carlo method. Finally, in section 5, is the brief discussion. Throughout this paper the geometric units  $G = C = K = 1$  are used.

## 2 DESCRIPTION OF MODEL

In our accretion disc-corona system, a geometrically thin and optically thick disc is sandwiched by a magnetic corona, and part of the gravitational energy of the accreted matter is released in the hot corona. The general relativistic model for a steady, axisymmetric, and thin Keplerian disc around a Kerr black hole has been described in detail by NT73 and PT74. In their model, it has been assumed that there is no stress at disc's inner edge. The equation of angular momentum conservation is given as follows

$$[\dot{M}L^+ - 2\pi e^{\nu+\psi+\mu}W]_{,r} = 4\pi e^{\nu+\psi+\mu}QL^+, \quad (1)$$

where  $\dot{M}$  is the accretion rate of the disc,  $\nu$ ,  $\psi$ ,  $\mu$  are the metric coefficients,  $W$  is integrated shear stress,  $L^+$  is the specific angular momentum of a particle in the disc.

The total gravitational power dissipated in unit surface area of the disc-corona system  $Q$  is given by

$$Q = (\dot{M}/4\pi)e^{-(\nu+\psi+\mu)}f, \quad (2)$$

where the function of radius  $f$  is defined by PT74. In the case of "no-torque inner boundary condition", the boundary condition on  $f$  at the radius  $r_{ms}$  of marginally stable orbit is  $f_{ms} = 0$ .

If it is taken into account that magnetic stresses exert a torque on the inner edge of the accretion disc, the appropriate boundary condition at  $r_{ms}$  is expressed as (Agol & Krolik 2000)

$$f_{ms} = \frac{3}{2} \frac{\Delta\epsilon}{\chi_{ms}^2 C(r_{ms})^2} \quad (3)$$

where  $\Delta\epsilon$  is the additional radiative efficiency,  $\chi_{ms} = \sqrt{r_{ms}/M}$ , and  $C$  is general relativistic correction factor defined by PT74.

Using this boundary condition we have the new function  $f$  of radius, that is

$$f = -\frac{d\Omega}{dr}(E^+ - \Omega L^+)^{-2} \left[ \int_{r_{ms}}^r (E^+ - \Omega L^+) \frac{dL^+}{dr} dr - \frac{3(E_{ms} - \Omega_{ms} L_{ms}^+)^2 \Delta\epsilon}{2\Omega_{ms} \chi_{ms}^2 C_{ms}^{1/2}} \right]. \quad (4)$$

$E^+$  and  $L^+$  are the specific energy and the specific angular momentum of a particle in the disc, respectively, and they read

$$E^\dagger = (1 - 2\chi^{-2} + a_*\chi^{-3}) / (1 - 3\chi^{-2} + 2a_*\chi^{-3})^{1/2}, \quad (5)$$

$$L^\dagger = M\chi(1 - 2a_*\chi^{-3} + a_*^2\chi^{-4}) / (1 - 3\chi^{-2} + 2a_*\chi^{-3})^{1/2}. \quad (6)$$

$\chi = \sqrt{r/M}$  is the dimensionless radial coordinate, and  $a_* = a/M$  is the dimensionless black hole spin parameter.

The power dissipated in the corona (i.e. the magnetic Poynting flux in the vertical direction from the thin disc) is

$$Q_{cor} = P_m v_P = \frac{B^2}{8\pi} v_P \quad (7)$$

where  $P_m$  is the magnetic pressure in the disc, and  $v_P$  is the velocity of magnetic flux transported vertically in the disc. Here we assume the velocity  $v_P$  of magnetic flux tubes is proportional to their internal Alfvén velocity, i.e.  $v_P = b v_A$ , and  $b$  is related to the efficiency of buoyant transport of magnetic structure in the vertical direction inside the disc, which is of the order of unity for extremely evacuated tubes (Merloni & Fabian 2002).

Now we give the equations of the disc structure as follows. The equation of vertical pressure balance in the vertically-averaged form is (Novikov & Thorne 1973)

$$H = (P/\rho)^{1/2} (r^3/M)^{1/2} AB^{-1} C^{1/2} D^{-1/2} E^{-1/2} \quad (8)$$

where  $H$  is the height of the accretion disc,  $P$  and  $\rho$  are pressure and density of the disc respectively.  $A, B, C, D, E$  are general relativistic correction factors defined as follows:

$$\begin{cases} A = 1 + a_*^2 \chi^{-4} + 2a_*^2 \chi^{-6} \\ B = 1 + a_* \chi^{-3} \\ C = 1 - 3\chi^{-2} + 2a_*^2 \chi^{-3} \\ D = 1 - 2\chi^{-2} + a_*^2 \chi^{-4} \\ E = 1 + 4a_*^2 \chi^{-4} - 4a_*^2 \chi^{-6} + 3a_*^4 \chi^{-8} \end{cases} \quad (9)$$

The equation of energy conservation is (see Eq.(5.6.13) in NT73)

$$W = \frac{4}{3} (M/r^3)^{-1/2} CD^{-1} Q, \quad (10)$$

and  $W$  is integrated shear stress defined as

$$W = 2 \int_0^h t_{r\varphi} dz \sim 2t_{r\varphi} H, \quad (11)$$

where  $t_{r\varphi}$  is the interior viscous stress in the disc.

The equation of state for gas on the disc is

$$P = P_{mag} + P_{tot} = P_{mag} + \frac{1}{3} a T^4 + \rho_0 (T/m_p) \quad (12)$$

where  $P_{tot}$  is the total pressure (gas pressure plus radiation pressure) at disc mid-plane,  $a$  is the radiative constant.  $m_p$  is the rest mass of proton,  $\rho_0$  and  $T$  are the density of rest mass and the temperature in the disc, respectively.

In the SSD model the interior viscous stress  $t_{r\varphi}$  is usually assumed to be proportional to the pressure, i.e.

$$t_{r\varphi} = \alpha P. \quad (13)$$

Since the process of generating magnetic fields in the accretion disc is still unclear, we adopted different magnetic pressures as:

$$P_{mag} \simeq \begin{cases} \alpha_0 P_{tot} = \alpha_0 (P_{gas} + P_{rad}) \\ \alpha_0 P_{gas} \\ \alpha_0 \sqrt{P_{gas} P_{tot}} \end{cases}, \quad (14)$$

and as  $\alpha_0$  is a constant of the order of unity, we adopt  $\alpha_0 = 1$  in our calculations.

In the disc-corona scenario, the soft photons from the disc are scattered by the electrons in the corona to X-ray bands. About half of the scattered photons are intercepted by the disc. It is a rough approximation because light bending effects ought to be taken into account at the vicinity of BH. The reflection albedo  $a_0$  is relatively low ( $a_0 \sim 0.1 - 0.2$ ), and most of the incident photons from the corona are re-radiated as black body radiation (Zdziarski et al. 1999). Thus the energy transport equation for the disc is

$$\alpha T^4 = 2\kappa H \rho (Q - Q_{cor} + \frac{1 - a_0}{2} Q_{cor}), \quad (15)$$

where  $\kappa$  is the Rosseland mean of total opacity which can be expressed as

$$\kappa = (0.64 \times 10^{23}) \rho T^{-7/2} + 0.40 \quad (cm^2/g), \quad (16)$$

and  $a_0 = 1.5$  is adopted in the calculations.

Solving equations (2),(7)-(16) numerically, the power dissipated in the corona  $Q_{cor}$  and the structure of the disc can be derived as function of  $r$ . The ratio of the power dissipated in the corona to the total for such disc-corona system is given as

$$\langle f \rangle = \frac{\int Q_{cor} 2\pi (\varpi \rho / \sqrt{\Delta})_{\theta=\pi/2} dr}{\int Q 2\pi (\varpi \rho / \sqrt{\Delta})_{\theta=\pi/2} dr}, \quad (17)$$

the concerned Kerr metric coefficients are given by (Thorne et al. 1986)

$$\begin{cases} \varpi = (\Sigma/\rho) \sin \theta, \Sigma^2 \equiv (r^2 + a^2)^2 - a^2 \Delta \sin^2 \theta, \\ \rho^2 \equiv r^2 + a^2 \cos^2 \theta, \Delta \equiv r^2 + a^2 - 2Mr. \end{cases} \quad (18)$$

### 3 NUMERICAL RESULTS

By using Eq.(2)-(6) we have the total gravitational power  $Q$  versus the radius of the disc for the different values of  $\Delta\varepsilon$  as shown in Fig.1. Note that the power  $Q$  is in units of  $Q_0 = \dot{M}/M^2$ , where  $M$  is the BH mass. Inspecting the above Fig, we have the following results: (I) the power  $Q$  depends sensitively on the values of  $\Delta\varepsilon$ , i.e. the magnetic torque can considerably enhance the amount of energy  $Q$  released in the disc; (II) the power  $Q$  decreases monotonically with the increasing radius, it indicates that the energy flux mostly comes from the inner region of the disc.

The ratio of accretion power dissipated into the corona  $\langle f \rangle$  as functions of the parameter  $\Delta\varepsilon$  and the dimensionless BH spin parameter  $a_*$  are shown in Fig.2 and Fig.3(a), and the magnetic pressure  $P_{mag} = \alpha_0 P_{tot}$  is adopted in our calculations. From the above Fig.2 and Fig.3(a), we find that the global value of  $\langle f \rangle$  is insensitive on the parameter  $\Delta\varepsilon$  for  $\Delta\varepsilon > 1$ , but the global value increases with the increasing the spin parameter  $a_*$ . The curves of  $\langle f \rangle$  versus accretion rate  $\dot{m}$  for the deferent BH spin parameter  $a_*$  are plotted in Fig.3(b). The dimensionless accretion rate  $\dot{m}$  is defined as  $\dot{m} = \dot{M}/\dot{M}_{Edd}$  in the calculations. As shown in Fig.3b

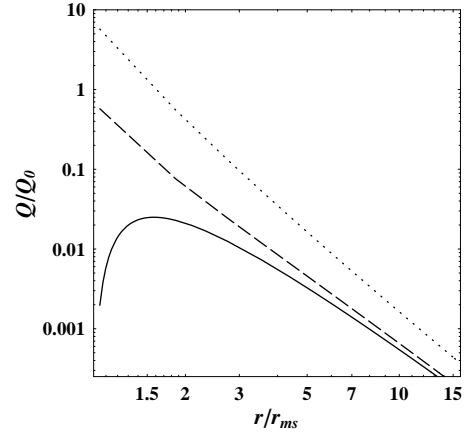


**Figure 1.** The value of  $Q/Q_0$  varying with  $r/r_{ms}$  for the different values of  $\Delta\varepsilon$ :  $\Delta\varepsilon = 0$  (solid lines),  $\Delta\varepsilon = 0.1$  (dashed lines),  $\Delta\varepsilon = 1$  (dotted lines); The dimensionless BH spin parameter  $a_* = 0.95$  is assumed.

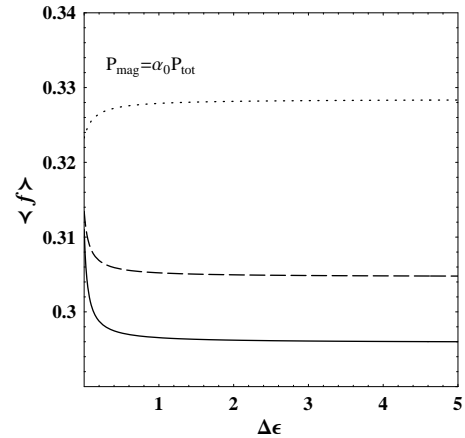


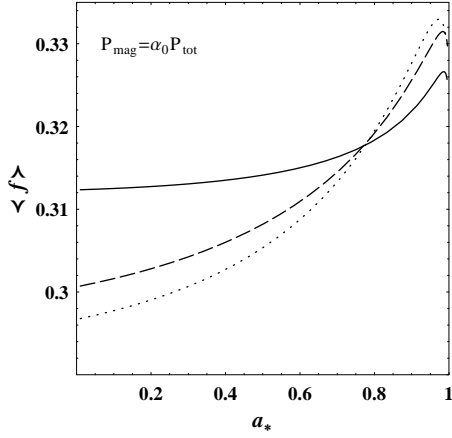
**Figure 2.** The global value of  $\langle f \rangle$  as a function of the parameter  $\Delta\varepsilon$  for three different values of  $a_*$ :  $a_* = 0$  (solid lines),  $a_* = 0.5$  (dashed lines),  $a_* = 0.9$  (dotted lines).  $\dot{m} = 0.1$ ,  $\alpha = 0.3$  is adopted in the calculations.

the global value  $\langle f \rangle$  is independent of accretion rate  $\dot{m}$  for a given BH spin parameter  $a_*$  if the magnetic pressure  $P_{mag} = \alpha_0 P_{tot}$  is adopted. We find that this result is consistent with those in Cao (2008), though the central black hole is Kerr black hole in our model, while a Schwarzschild black hole in Cao (2008).

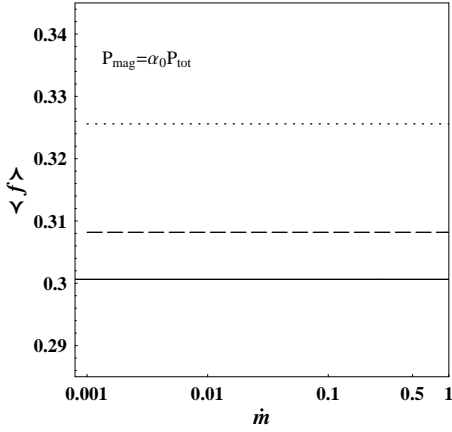
We plot the curves of the global value  $\langle f \rangle$  versus different parameters with  $P_{mag} = \alpha_0 P_{gas}$  and  $P_{mag} = \alpha_0 \sqrt{P_{gas} P_{tot}}$  in Fig 4 and Fig 5, respectively.

Inspecting the Fig.4 and Fig.5 we find that our disc-corona model calculations with  $P_{mag} = \alpha_0 P_{gas}$  show the integration fraction of accretion power dissipated into the corona  $\langle f \rangle \sim 0.270 - 0.298$  with the BH spin parameter  $a_* \sim 0.01 - 0.998$ , and the model with  $P_{mag} = \alpha_0 \sqrt{P_{gas} P_{tot}}$  shows that  $\langle f \rangle \sim 0.285 - 0.315$  with the BH spin parameter  $a_* \sim 0.01 - 0.998$  at  $\dot{m} < 0.05$ , for different values of  $\Delta\varepsilon$ .

From Fig.4(a) we find that the values of  $\langle f \rangle$  depend on the parameters  $a_*$  and  $\Delta\varepsilon$  when  $\Delta\varepsilon < 1$ .  $\langle f \rangle$  decreases (increases) as  $\Delta\varepsilon$  changes from 0 to 1, for  $a_* < 0.4$  ( $a_* > 0.4$ ). In fact, the magnetic fields connecting the plunging region to the disc can



(a)



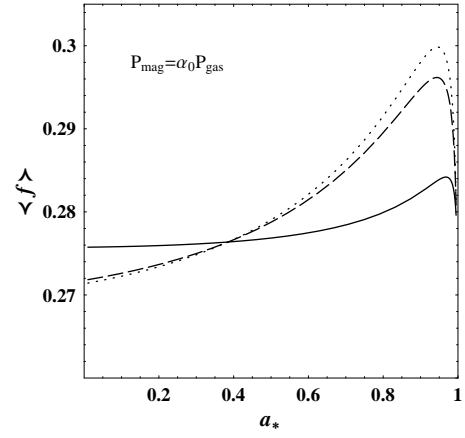
(b)

**Figure 3.** (a) The global value of  $\langle f \rangle$  varies with  $a_*$  for different values of  $\Delta\varepsilon$ :  $\Delta\varepsilon = 0$  (solid lines),  $\Delta\varepsilon = 0.1$  (dashed lines),  $\Delta\varepsilon = 1$  (dotted lines).  $\dot{m} = 0.1$  is adopted in the calculations, (b) The global value of  $\langle f \rangle$  varies with  $\dot{m}$  for different values of  $a_*$ :  $a_* = 0$  (solid lines),  $a_* = 0.5$  (dashed lines),  $a_* = 0.9$  (dotted lines),  $\Delta\varepsilon = 0.1$  and  $\alpha = 0.3$  are adopted in the calculations.

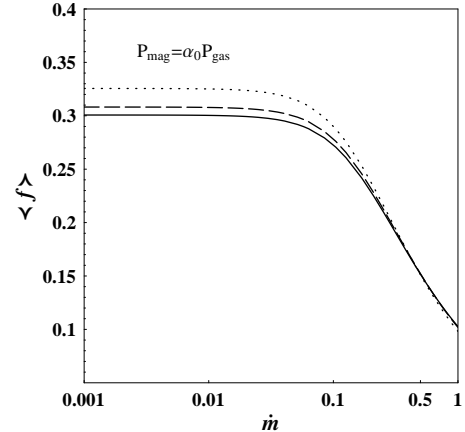
exert stresses on the inner edge of the disc and transfer energy from the plunging region to the disc-coronae system. So the values of  $Q_{\text{cor}}$  and  $Q$  all increase with the increasing  $\Delta\varepsilon$ .  $Q_{\text{cor}}$  and  $Q$  are also positively correlated to BH spins. For  $a_* < 0.4$ , the value of  $Q_{\text{cor}}$  increases more slowly than that of  $Q$  with the increasing  $\Delta\varepsilon$ . Thus the ratio of accretion power dissipated into the corona,  $\langle f \rangle$ , decreases with the increasing  $\Delta\varepsilon$ . For  $a_* = 0.4$ , we find that the change of the magnetic torque has no influence on the ratio of the power dissipated in the corona to the total power. This critical BH spin parameter is about  $a_* = 0.78$  in Fig.3(a), and is about  $a_* = 0.6$  in Fig.5(a).

In addition, it should be noted that the value of  $\langle f \rangle$  is also insensitive on the  $\Delta\varepsilon$  for  $\Delta\varepsilon > 1$ , as  $P_{\text{mag}} = \alpha_0 P_{\text{gas}}$  or  $P_{\text{mag}} = \alpha_0 \sqrt{P_{\text{gas}} P_{\text{tot}}}$  is adopted in our calculations.

As shown in Fig.4(b) and Fig.5(b), the value  $\langle f \rangle$  decreases monotonically with the increasing accretion rate for  $\dot{m} \geq 0.05$ .  $\langle f \rangle$  can reach  $\sim 0.3$  at the lower accretion rates. So it seems that the low luminosity BH can be fitted by our disc-corona model nicely. Merloni & Fabian (2002) also proposed that the magnetic



(a)



(b)

**Figure 4.** (a) The global value of  $\langle f \rangle$  varies with  $a_*$  for different values of  $\Delta\varepsilon$ :  $\Delta\varepsilon = 0$  (solid lines),  $\Delta\varepsilon = 0.1$  (dashed lines),  $\Delta\varepsilon = 1$  (dotted lines).  $\dot{m} = 0.1$  is adopted in the calculations, (b) The global value of  $\langle f \rangle$  varies with  $\dot{m}$  for different values of  $a_*$ :  $a_* = 0$  (solid lines),  $a_* = 0.5$  (dashed lines),  $a_* = 0.9$  (dotted lines),  $\Delta\varepsilon = 0.1$  and  $\alpha = 0.3$  are adopted in the calculations.

corona should be stronger at low accretion rates, and their strength depends upon the nature of magnetic dissipation inside the disc.

#### 4 SIMULATION OF DISC SPECTRUM

In the disc-corona scenario, the comptonized spectrum has been computed by some authors using different approaches in previous works. Two kinds of approaches are used in order to get the emergent spectrum. One of common approaches is to solve the radiative transfer equation either numerically or analytically (Sunyaev & Titarchuk 1980; Poutanen & Svensson 1996). Another kind of approach is the Monte Carlo simulation (Pozdnyakov et al. 1983; Gorecki & Wilczewski 1984; Stern et al. 1995; Hua 1997; Ma et al. 2006). Recently, Ma et al. (2006) got the output spectra in the cases with and without the magnetic coupling effects (Li 2000, Li & Paczyński 2000, Li 2002a, Li 2002b) by using the Monte Carlo simulation.

In this paper, the steps of our simulations are: (i) sample a

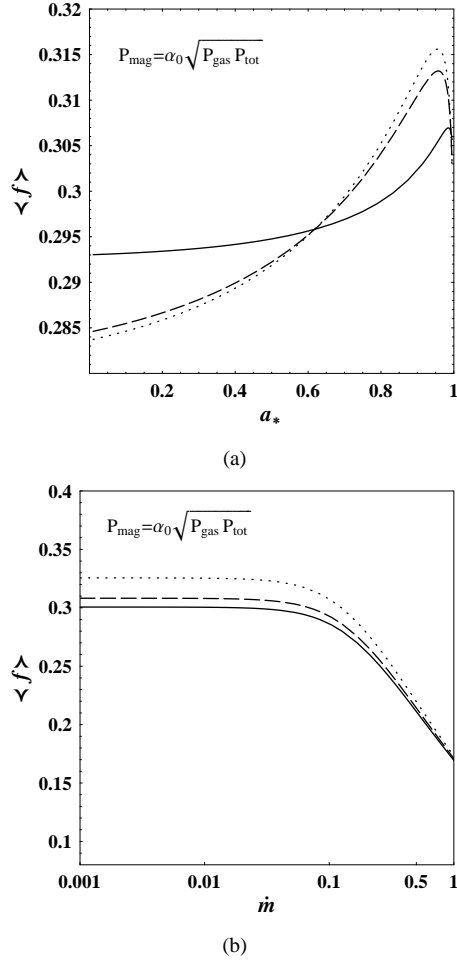


**Figure 5.** (a) The global value of  $\langle f \rangle$  varies with  $a_*$  for different values of  $\Delta\varepsilon$ :  $\Delta\varepsilon = 0$  (solid lines),  $\Delta\varepsilon = 0.1$  (dashed lines),  $\Delta\varepsilon = 1$  (dotted lines).  $\dot{m} = 0.1$  is adopted in the calculations, (b) The global value of  $\langle f \rangle$  varies with  $\dot{m}$  for different values of  $a_*$ :  $a_* = 0$  (solid lines),  $a_* = 0.5$  (dashed lines),  $a_* = 0.9$  (dotted lines),  $\Delta\varepsilon = 0.1$  and  $\alpha = 0.3$  are adopted in the calculations.

seed photon from the cold disc; (ii) draw a value for its free path and test whether it can leave the disc or corona; (iii) simulate the interaction of the photon with the medium; (iv) repeat steps (ii), (iii) till the photon leaves the system of the corona and disc.

In our disc-corona scenario, the dissipated power in the unit area of the disc,  $F$  is related to  $Q$  by  $F = Q - Q_{cor}$ , and according to Stefan-Boltzmann law we have the local effective temperature on the disc expressed by

$$T_d(r) = (F/\sigma_{SB})^{1/4}, \quad (19)$$

where  $\sigma_{SB}$  is the Stefan-Boltzmann constant. The local radiation spectrum is defined by the Planck function:

$$B_\nu(r) = \frac{2h}{c^2} \frac{\nu^3}{\exp[h\nu/kT_d(r)] - 1}, \quad (20)$$

thus the multicolor black-body spectrum of the disc is

$$L_\nu = \int_{r_{in}}^{r_{out}} B_\nu(r) 2\pi r dr. \quad (21)$$

The probability density of the seed photons can be written as

$$P(r, E) = \tilde{P}(r)P(E), \quad (22)$$

where  $\tilde{P}(r) = L(r)dr/L$  is the probability of a photon emitted in the ring  $r \sim r + dr$ , and  $L$  is the total luminosity of the disc.  $P(E)$  is the number density of photons having an energy  $E = h\nu$  that is given by Pozdnyakov et al. (1983)

$$P(E) = \frac{1}{2\zeta(3)} b^3 E^2 (e^{bE} - 1)^{-1}, \quad (23)$$

where  $b = 1/T_d$ ,  $\zeta(3) = 1.202$  is the Riemann Zeta function.

In our simulations, if the seed photon is scattered by the electron in the corona, the optical depth that the photon travels between the  $i$ -th and  $(i+1)$ -th scatterings can be drawn with  $\tau_i = -\ln \lambda$ , where  $0 \leq \lambda \leq 1$  is a random number corresponding to a random event. The free path of photon can be drawn with

$$\frac{\tau_i}{n_e \sigma} = \frac{-\ln \lambda \sigma_T H_c}{\sigma \tau_c}, \quad (24)$$

where  $n_e$ ,  $\sigma$  and  $\sigma_T = 6.65 \times 10^{-24} \text{ cm}^2$  are the number density of the electrons, cross-sections of scattering and Thomson scattering, respectively.  $H_c$  and  $\tau_c$  are the vertical height and optical depth of the corona. Since the electrons in the hot corona are relativistic, the cross-section of scattering  $\sigma$  depends not only on the energy of the photon but also on the energy and direction of the electron. So we use the cross-section averaged over the distribution of the electrons in Hua (1997) to draw the free path of the photon.

In the disc-corona system, hard X-ray photons irradiating the disc from the corona can be absorbed by the atoms in the disc, as well as being scattered by the free electrons. In this case, we choose the lesser of the two free paths that are drawn with  $\sigma_a$  and  $\sigma_s$  to draw the free path of the photon, where  $\sigma_a$  and  $\sigma_s$  are respectively the cross sections of absorption and scattering. The cross sections of absorption  $\sigma_a$  is taken from Morrison & McCammon (1983), and the cross sections of scattering can be given by the Klein-Nishina formula

$$\sigma_s = \frac{3\sigma_T}{4\varepsilon} \left[ \left(1 - \frac{4}{\varepsilon} - \frac{8}{\varepsilon^2}\right) \ln(1 + \varepsilon) + \frac{1}{2} + \frac{8}{\varepsilon} - \frac{1}{2(1 + \varepsilon)^2} \right], \quad (25)$$

where  $\varepsilon$  is the energy of the incident photon in unit of electron-rest-energy.

As the free path is known, the position that the photon arrives before the next interaction can be calculated. If the photon is outside the disc-corona system, it will escape away from the system and its energy and direction are recorded. If the photon transfers from the disc to the corona or inverse, the point where the trajectory of the photon cross the interface between the disc and corona will be regarded as the next initial position of the photon in calculations.

In the simulating the interaction of photon and electron, we can sample a electron from thermal distribution, then calculate the energy and direction of scattered photon. In the calculation, we follow the calculation procedure described in P83. The bound-free absorption of hard X-rays by the atoms in the disk will lead to ionization and vacancy, and induce emission of fluorescence lines with the probability called fluorescence yield,  $Y$ . In our simulations, if the photon is absorbed by a certain atom or ion, we can draw a random number  $\lambda$  ( $0 \leq \lambda \leq 1$ ) and compare it with the corresponding fluorescence yield. If  $\lambda \leq Y$ , an emission line is brought out, whose direction can be sampled from the isotropic distribution. If  $\lambda > Y$ , the photon vanishes and its trajectory ends. We only consider the 6.4 keV Fe  $K_\alpha$  fluorescence line in our simulations, due

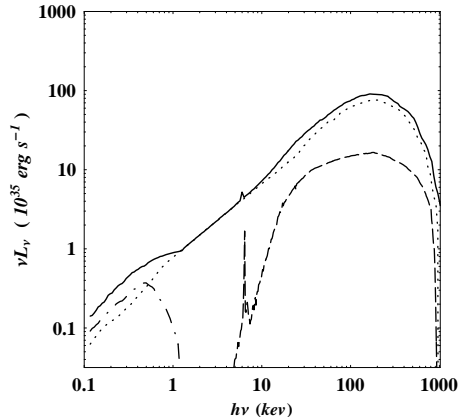


**Figure 6.** The emerged spectrum from the disc-corona system. The total emissive spectrum and its black body, power-law and reflected components are shown in solid, dot-dashed, dotted and dashed lines, respectively. The radii of the inner and outer edges of the corona are taken as  $r_{in} = r_{ms}$  and  $r_{out} = 100r_{ms}$ , and  $a_* = 0.998$ ,  $\Delta\epsilon = 0.1$  and  $\dot{m} = 0.05$  are adopted in the calculations.

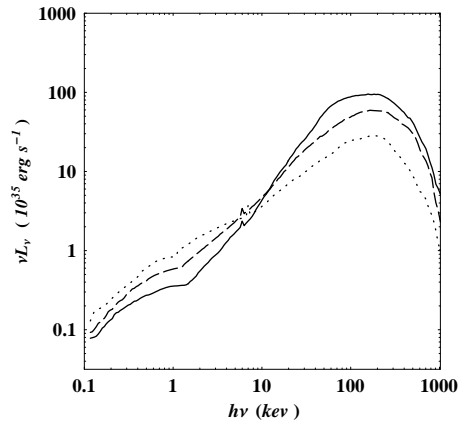
to the large abundance and cross-section of absorption of iron. If the energy of the absorbed photon is less than the iron K-shell absorption edge, i.e.  $E < 7.1$  keV, no emission line is produced, while Fe  $K_\alpha$  lines emanate with  $Y = 0.34$  for  $E > 7.1$  keV (Ma et al. 2006).

In our simulations, the half height of the disc is assumed to be  $H = 0.05r_{ms}$ . All the spectra in this paper are given in forms of curves rather than histogram to make the curves look smooth. Fortran 95 is used in the calculations and Mathematica 7.0 software is adopted to plot the figures.

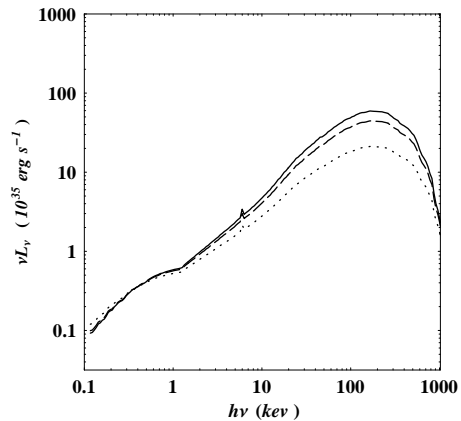
The typical results for the spectra of our Monte Carlo simulations are given in Fig. 6. The spectrum of the disc-corona system comprises three components, the black-body spectrum formed by unscattered photons, the power-law spectrum formed by photons that escape from the corona after several times of inverse Compton scatterings, and the reflected spectrum characterized by the iron fluorescence line and reflection hump.

Spectra with different coronal geometry parameters are given in Fig. 7. We simulate spectra with different heights of corona:  $H_C = 0.5r_{ms}$ ,  $H_C = r_{ms}$ ,  $H_C = 2r_{ms}$ , in Fig. 7(a). It is found that the spectra steepen in the 2-200 keV range with the increasing height of corona. This result can be explained as follows: when the corona becomes thicker, the amount of photon-electron scattering increases, and the energy of the escaped photons increases. Therefore, hardening of the spectrum is anticipated. We present the spectra with different radii of the outer edge of the corona:  $r_{out} = 100r_{ms}$ ,  $r_{out} = 50r_{ms}$ ,  $r_{out} = 20r_{ms}$  in Fig. 7(b). The fluxes increase with  $r_{out}$ , since a larger disc can lead to more energy from the coronal surface. The spectral profile changes slightly in this case.

Spectra with different accretion rates  $\dot{m}$ ,  $\Delta\epsilon$  and BH spin parameters  $a_*$  are given in Fig. 8. From Fig. 8(a) we find that the fluxes increase as  $\dot{m}$  changes from 0.01 to 0.1, and the spectral profile changes obviously. As the accretion rate  $\dot{m}$  increases, the total gravitational energy dissipated is enhanced remarkably. In this case, more seed photons escape from the surface of the disc; these photons also have higher energies. It is found in Fig. 8(b) that the fluxes increase as  $\Delta\epsilon$  increases from 0.1 to 2, since the



(a)



(b)

**Figure 7.** The simulated spectra of the disc-corona system. (a) Solid, dashed, and dotted lines correspond to the spectra with different heights of corona:  $H_C = 2r_{ms}$ ,  $H_C = r_{ms}$ ,  $H_C = 0.5r_{ms}$ , for the radii of the inner and outer edges of the corona are taken as  $r_{in} = r_{ms}$  and  $r_{out} = 100r_{ms}$ . (b) Solid, dashed, and dotted lines correspond to the spectra with different radii of the outer edges of the corona:  $r_{out} = 100r_{ms}$ ,  $r_{out} = 50r_{ms}$ ,  $r_{out} = 20r_{ms}$ , for  $r_{in} = r_{ms}$  and  $H_C = r_{ms}$ .  $a_* = 0.5$ ,  $\Delta\epsilon = 0.1$  and  $\dot{m} = 0.05$  are adopted in the calculations.

magnetic torque can transfer energy from the plunging region to the disc-corona system. The energy distribution of the seed photons, hence the emerged spectrum, also changes in this case. From Fig. 8(c) we see that the fluxes increase with  $a_*$ . Indeed, as  $a_*$  increases the inner edge of disc approaches the BH horizon  $r_H = M(1 + \sqrt{1 - a_*^2})$ , and more gravitational energy can be released.  $M = 10M_\odot$ , and  $P_{mag} = \alpha_0 \sqrt{P_{gas} P_{tot}}$  is adopted through the calculations.

## 5 DISCUSSION

In this work, we propose a disc-corona model, in which magnetic fields exert a torque on the inner edge of the accretion disc, and part of gravitational energy is dissipated in the hot corona. The total gravitational power  $Q$  is derived from the thin-disc dynamics

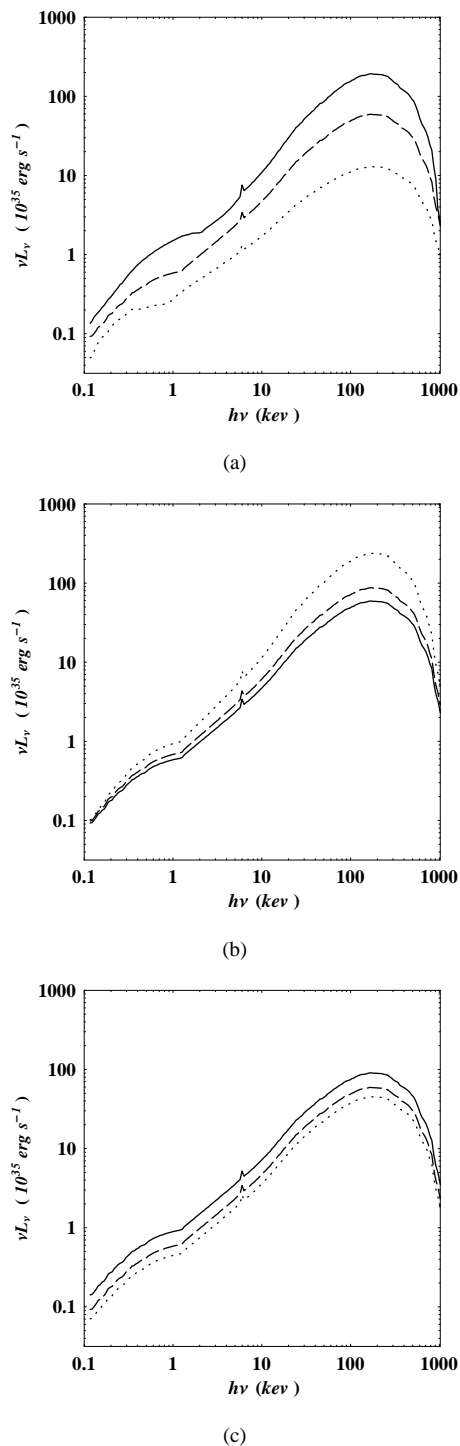


**Figure 8.** The simulated spectra of the disc-corona system. (a) Solid, dashed, and dotted lines correspond to the spectra with different accretion rates :  $\dot{m} = 0.1$ ,  $\dot{m} = 0.05$ ,  $\dot{m} = 0.01$ , for  $a_* = 0.5$ ,  $\Delta\varepsilon = 0.1$ ; (b) Solid, dashed, and dotted lines correspond to the spectra with different  $\Delta\varepsilon$  :  $\Delta\varepsilon = 0.1$ ,  $\Delta\varepsilon = 1$ ,  $\Delta\varepsilon = 2$ , for  $a_* = 0.5$ ,  $\dot{m} = 0.05$ ; (c) Solid, dashed, and dotted lines correspond to the spectra with different spin parameters :  $a_* = 0.998$ ,  $a_* = 0.5$ ,  $a_* = 0.1$ , for  $\dot{m} = 0.05$ ,  $\Delta\varepsilon = 0.1$ .  $H_C = r_{ms}$ ,  $r_{in} = r_{ms}$  and  $r_{out} = 100r_{ms}$  are adopted in the calculations.

equations and the global solutions are obtained numerically. It is found that the fraction of the power dissipated into the corona in the total for such disc-corona system increases with the increasing the dimensionless black hole spin parameter  $a_*$ , but is insensitive on the parameter  $\Delta\varepsilon$  for  $\Delta\varepsilon > 1$ .

We simulate the emerged spectra from the disc-corona system for the different parameters using the Monte-Carlo method. It is found that the spectral profile changes obviously with varying the height of the corona and the accretion rate of the disc. The reasonable geometry of the corona is important for simulating the emerged spectra using the Monte-Carlo method. We adopt a slab corona in this paper. However the geometry of the corona is still matter of debate, e.g. Stern et al. (1995) proposed a patchy corona that made of a number of separate active regions. Furthermore, the observed correlation between the photon index and the reflection strength Zdziarski et al. (1999) has demonstrated the need for further geometrical/dynamical parameters, such as the relativistic bulk motion velocity of the coronal material (Malzac et al. 2001).

Our model needs to be improved in other aspects. For example, the gravitational effects on the trajectories of photons need to be taken into account, the cooling of synchrotron radiation should be considered and the ray-tracing should be used in our calculations.

The magnetic pressure  $P_{mag}$  plays an important role in our model. In fact we can get the magnetic energy density from the coronal power  $Q_{cor}$  as the coronal geometry is assumed. Then the small-scale magnetic field  $Q_{dynamo}$  in the corona can be derived from the magnetic energy density.

On the other hand, models and simulations of jet production (Blandford & Znajek 1977; Blandford & Payne 1982; Meier 1999) show that it is the poloidal component of the large-scale magnetic field which mainly drives the production of powerful jets. Several theoretical models have been proposed for acceleration and collimation of jets, which can be divided into two main regimes, the Poynting flux regime and the hydromagnetic regime. Both regimes are related to a poloidal magnetic field threading the disc or BH, from which energy and angular momentum are extracted. In the Poynting flux regime, energy is extracted in Poynting flux (i.e. purely electromagnetic energy), but in the form of magnetically driven material winds in the latter regime. Furthermore, some authors have agreed that jet formation should involve an accretion disc threaded by a large-scale magnetic field (Livio et al. 1999; Meier 1999).

Though the origin of large-scale magnetic field is still under controversy, some previous works (Tout & Pringle 1996; Romanova et al. 1998) have proposed that the large-scale field can be produced from the small-scale field created by dynamo processes. The length scale of the fields created by dynamo processes is of the order of the disc thickness  $H$ , and the poloidal component of the magnetic field is given approximately by

$$B_P \sim (H/r)B_{dynamo}, \quad (26)$$

If the field is created in the thin accretion discs ( $H \ll r$ ), the large-scale field is very weak. For the ADAF cases, the disc thickness  $H \sim r$  and the poloidal component of the magnetic field shall be stronger. In our disc-corona scenario, the energetically dominant corona are the ideal sites for launching the powerful jets/outflows (Merloni & Fabian 2002). The large-scale magnetic fields created by dynamo processes in the corona are significantly stronger than the thin disc due to the corona being much thicker than the cold, thin disc. So the corona can power a stronger jet than the thin disc.

We shall discuss the acceleration of jet in the Poynting flux regime and the hydromagnetic regime in future work.

#### ACKNOWLEDGMENTS

This work is supported by the National Basic Science Foundation of China under the Distinguished Young Scholar Grant 10825313, the National Basic Research Program of China (2009CB4901) and the Project for Excellent Young and Middle-Aged Talent of Education Bureau of Hubei Province under Grant Q200712001. We are very grateful to the anonymous referee for his/her helpful comments on the manuscript.

#### REFERENCES

- Agol E., Krolik J. H., 2000, *ApJ*, 528, 161  
 Balbus, S.A. & Hawley, J.F. 1998, *Revs. Mod. Phys.*, 70, 1  
 Blandford R. D. & Znajek R. L., 1977, *MNRAS*, 179, 433  
 Blandford R. D. & Payne D. G., 1982, *MNRAS*, 199, 883  
 Cao, X.-W. 2008, *ApJ*, 613, 716  
 Gammie. C. & Charles, F. 1999, *ApJL*, 522, 57  
 Gorecki, A. & Wilczewski, W. 1984, *Acta Astron.*, 34, 141  
 Hua, X. M. 1997, *Computers in Physics*, 11, 660  
 Ionson, J. A. & Kuperus, M. 1984, *ApJ*, 284, 389  
 Krolik, J.H. 1999, *ApJ*, 515, L73  
 Li, L.-X. 2000, *ApJ*, 533, L115  
 Li, L.-X. 2002a, *ApJ*, 567, 463  
 Li, L.-X. 2002b, *A&A*, 392, 469  
 Li, L.-X. Paczyński, B. 2000, *ApJ*, 534, L197  
 Liang, E. P. & Price, R. H. 1977, *ApJ*, 218, 247  
 Liu B.-F., Mineshige S. & Shibata K., 2002, *ApJ*, 572, L173  
 Livio M., Ogilvie G. I., Pringle J. E., 1999, *ApJ*, 512, 100  
 Ma R.-Y., Wang, D.-X., Zuo X.-Q. 2006, *A&A*, 453, 1  
 Malzac J., Beloborodov A., Poutanen J., 2001, *MNRAS*, 326, 417  
 Meier, D. L. 1999, *ApJ*, 522, 753  
 Merloni A. & Fabian A. C., 2002, *MNRAS*, 332, 165  
 Morrison, R., & McCammon, D. 1983, *ApJ*, 270, 119  
 Narayan, R. & Yi, I., 1994, *ApJ*, 428, 13  
 Narayan R. & Yi I., 1995, *ApJ*, 452, 710  
 Novikov I. D., & Thorne, K. S., 1973, in *Black Holes*, ed. C. Dewitt & B. S. Dewitt (New York: Gordon and Breach) (NT73)  
 Page D. N. & Thorne K. S., 1974, *ApJ*, 191, 499 (PT74)  
 Pozdnyakov, L. A., Sobol, I. M., Sunyaev, R. A. 1983, *Ap&SS Rev.* 2, 189, 83  
 Poutanen, J., & Svensson, R. 1996, *ApJ*, 470, 249  
 Romanova M. M., Ustyugova G. V., Koldoba A. V., Chechetkin V. M., & Lovelace R. V. E., 1998, *ApJ*, 500, 703  
 Shakura, N.I. & Sunyaev, R.A. 1973, *MNRAS* 24, 337  
 Stern, B. E., Begelman, M. C., Sikora, M. 1995, *MNRAS*, 272, 291  
 Sunyaev, R. A., & Titarchuk, L. G. 1980, *A&A*, 86, 121  
 Tout C. A., & Pringle J. E., 1996, *MNRAS*, 281, 219  
 Thorne K. S., Price R. H., Macdonald D. A., 1986, *Black Holes: The Membrane Paradigm*, Yale Univ. Press, New Haven  
 Zdziarski A. A., & Lubinski P., & Smith D.A., 1999, *MNRAS*, 303, L11